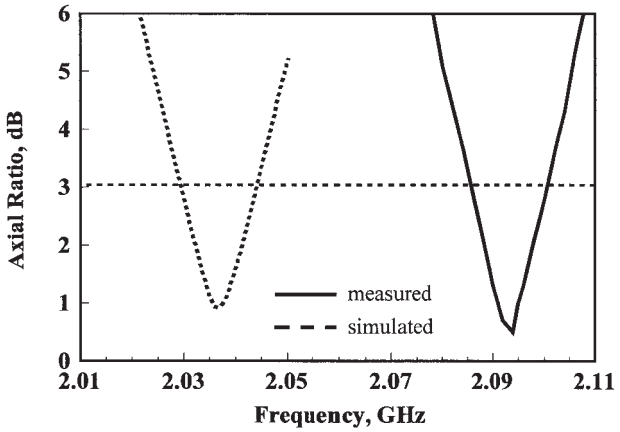

Figure 6 Measured axial ratio at the lower-frequency band of Antenna B

ing-frequency bands was constructed. In this case, Δl is set to be 0 mm, and the dimensions of s and d are selected to be 4 and 19.5 mm, respectively. The measured and simulated (by IE3D) return losses against frequency for antenna A are shown in Figure 2. Agreement between them is satisfactory, except for the slight frequency deviations that can mainly be due to the error of the substrate permittivity. From the experimental results, it is observed that 10-dB input-impedance bandwidths centered at 2090 and 5505 MHz are 1.9% and 9.8%, respectively, for the two operating frequency bands, which are due to the square-ring and rectangular microstrip antennas. The radiation patterns measured at 2090 and 5505 MHz are also plotted in Figures 3 and 4, respectively. The broadside radiation patterns are seen at the two operating frequencies. The peak gain is about 4.2 dBi for the square-ring microstrip antenna and 7.5 dBi for the rectangular microstrip antenna.

The prototype (antenna B) of the proposed dual-frequency microstrip antenna with dual polarization (CP/LP) radiations was also implemented. The dimensions of the square-ring and rectangular patches are the same as those of antenna A, except that $\Delta l =$ 4.6 mm. To achieve the impedance matching of the CP square-ring microstrip antenna, the dimensions of s and d are changed to 2 and 15 mm, respectively. Figure 5 presents the experimental results of Antenna B, together with the simulated results. The measured 10-dB input-impedance bandwidth is about 2.4% (with reference to the center frequency of 2094 MHz) for the CP square-ring microstrip antenna and 7.5% (referred to the center frequency 4980 MHz) for the LP rectangular microstrip antenna. It has to be noted that the center frequency of the rectangular microstrip antenna is decreased from 5505 (antenna A) to 4980 MHz (antenna B) is due to the changes of the feed position, which is necessary to achieve the impedance matching for the CP square-ring microstrip antenna. The axial ratio in the lower frequency band of antenna B is also measured and presented in Figure 6. The 3-dB axial-ratio CP bandwidth is about 0.7%. The radiation patterns at 4980 MHz for antenna B is similar to the results shown in Figure 4.

4. CONCLUSION

The dual-frequency microstrip antenna that can produce the identical linear polarization or dual polarizations at two operating-frequency bands has been proposed and the antenna prototypes are constructed and tested. The two resonant frequencies of the dual-frequency antenna are due to a square-ring microstrip antenna and a rectangular microstrip antenna, respectively. Hence, the broadside radiation patterns can be obtained in the two operating-frequency bands. The measured results have good agreements with the simulated results, which provide the experimental validation.

REFERENCES

1. J.Y. Jan, Low-profile dual-frequency circular microstrip antenna for dual ISM bands, Electron Lett 37 (2001), 999–1000.
2. K. Oh, B. Kim, and J. Choi, Design of dual and wideband aperture-stacked patch antenna with double-sided notches, Electron Lett 40 (2004), 643–645.
3. J.S. Row, Dual-frequency dual-polarised microstrip antenna fed by an inclined slot, Microwave Opt Technology Lett 41 (2004), 512–514.
4. J.S. Row and K.W. Lin, Low-profile design of dual-frequency and dual-polarised triangular microstrip antennas, Electron Lett 40 (2004), 153–154.
5. G. Mayhew-ridgers, J.W. Odendaal, and J. Joubert, New feeding mechanism for annular-ring microstrip antenna, Electron Lett 36 (2000), 605–606.
6. J.S. Row, Design of square-ring microstrip antenna for circular polarisation, Electron Lett 40 (2004), 93–94.

A SIGNAL- AND NOISE-MEASUREMENT PROCEDURE FOR AN ANTENNA/RF RECEIVER COMBINATION IN A SHORT-RANGE AUTOMOTIVE COMMUNICATION SYSTEM

Victor Rabinovich,[2] Basim Al-Khateeb,[1] Barbara Oakley,[3] and Nikolai Alexandrov[2]
[1] DaimlerChrysler Corporation
800 Chrysler Drive
Auburn Hills, Michigan
[2] Tenatronics Ltd.
776 Davis Drive
Newmarket, Ontario, Canada
[3] Department of Electrical and Systems Engineering
Oakland University
Rochester, Michigan

Received 13 April 2005

ABSTRACT: *A signal- and noise-measurement test procedure for an RF remote keyless entry (RKE) is presented. RKE systems are often designed for automotive applications, and include an RF receiver along with either an integrated antenna or a separately located external active antenna. Unlike previous methods, the new test procedure presented here allows measurement of the signal and noise levels at the output of an RKE system's RF receiver while the receiver is installed in its usual location on board the vehicle and connected with its antenna. This procedure also solves the problem of obtaining signal and noise measurements in systems with integrated receiver/antenna units.* © 2005 Wiley Periodicals, Inc. Microwave Opt Technol Lett 47: 116–119, 2005; Published online in Wiley InterScience (www.interscience.wiley.com). DOI 10.1002/mop.21097

Key words: *short-range communication; antenna; remote keyless entry (RKE) receiver; signal and noise measurements*

1. INTRODUCTION

A significant number of today's automobiles are purchased with the option of a remote keyless entry (RKE) system [1, 2]. Most automotive RKE systems serve to lock and unlock a vehicle's doors and trunk, as well as to help protect against theft. Some systems also include remote start and car-finder functions. RKE systems generally consist of a portable fob-key transmitter carried

by the vehicle's driver as well as a receiver unit mounted on the vehicle itself. RKEs most commonly use a frequency of 315 MHz in the United States, Canada, and Japan, and 433.92 MHz in Europe.

The fundamental challenge for keyless-entry design is extending the range of the system. In this regard, two principle parameters determine signal detection at the required range: (i) the signal level received by the RKE system and (ii) the noise level at the receiver output when the receiver is located in its everyday operating environment—which can include interference from multiple sources on the car. At the design phase, an RF engineer chooses an antenna system as well as a receiver with a sensitivity that can provide the required range. The antenna gain determines the signal level at the receiver input, and the receiver sensitivity determines the thermal noise level of the RKE system.

Detection of a signal embedded within noise is a statistical process. The RKE system detects a demodulated signal with a known probability of detection P_0 if the signal-to-noise ratio is more than the certain value q (P_0 is a function of q). The signal-to-noise ratio, as given by Eq. (1), forms the fundamental equation for range estimation [2]:

$$q = \frac{\alpha \cdot EIRP \cdot G_a}{D^n} \cdot \frac{1}{N}, \quad (1)$$

where $EIRP$ is the effective power radiated by the fob key (for example, FCC regulations limit the $EIRP$ power for 315 MHz to -12 dBm),

$$\alpha = \left(\frac{\lambda}{4 \cdot \pi}\right)^2,$$

λ is the wavelength (-22 dBm for 315-MHz frequency), n is the pass-loss exponent (2 in free space), and G_a is the antenna gain.

If the antenna is attached to an amplifier, the gain of an active antenna can be expressed as

$$G_a = G_{pas} \cdot G_{amp}, \quad (2)$$

where G_{pas} is the gain of the passive portion of the antenna, and G_{amp} is the antenna amplifier gain.

N is the total noise level received by the receiver; it is known that for the UHF band [3]:

$$N = k \cdot T \cdot B \cdot F_{amp} \cdot G_{amp} + N_{ext} + k \cdot T \cdot B \cdot (F_{rec} - 1), \quad (3)$$

where k is the Boltzman's constant, T is the ambient room temperature, B is the equivalent bandwidth of the measuring device, F_{amp} is the antenna amplifier gain, F_{rec} is the receiver noise figure, N_{ext} is the external noise from the different interference sources surrounding the antenna, and q is the signal to noise ratio that is needed for the stable decoding (we assume $q = 10$ dB for the probability of detection equal to 0.99).

As can be seen from Eq. (1), the communication range for an RKE system can be estimated if the following parameters are known: effective radiated power, operating frequency, receiving antenna gain G_{act}, path loss exponent, and noise level N.

A typical test procedure for the antenna-gain estimation involves use of a spectrum analyzer [4]. This procedure is very convenient for measurement of external antennas with cables. However, accurate gain measurements of antennas integrated with RF circuits are not easy to obtain with such a procedure due to the interference between the RF circuit-board elements and the antenna itself. Making things even more difficult, such an antenna does not have an output cable that can be connected to the spectrum analyzer. Moreover, some gain-related parameters (for example, noise level and path-loss exponent number) are unpredictable in a real environment. For example, simply having several different microprocessor-noise sources in the car can dramatically decrease the signal's range. Although noise-value estimation can be implemented according to the procedure described in [5], the method described in that reference uses an antenna with the cable connected to the receiver, with the output of the receiver is connected to the voltmeter. In summary, a new method for testing integrated antenna/receiver units would be a useful addition to research in this area.

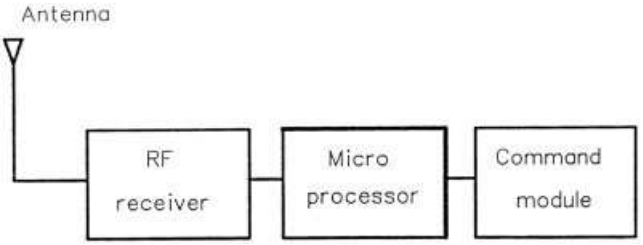

Figure 1 RKE-module architecture

This paper describes a simple way to evaluate signal and noise values received by an antenna and RF receiver of an RKE system in a real environment. The procedure is based on the method described in [5], but the main advance of our procedure is that the antenna and RF receiver can be left in their usual locations on the vehicle during the measurement period. Additionally, if the system for some unknown reason does not provide the required range, with this new procedure it is a straightforward task to determine which part of the system is causing the problem: the antenna with receiver, the noisy car equipment, or the digital processor. The secret to the procedure's effectiveness is in part based on its simplicity: a continuous-wave transmitter with an output-power level as specified by FCC regulations is first located at the customer-required range. Direct measurements of the signal and noise at the output of RF part of the RKE system can then be easily made.

2. RKE MODULE STRUCTURE

A typical RKE module structure is shown in Figure 1. It includes an antenna, an RF receiver, a microprocessor, and a command circuit. The RF receiver in the vehicle captures the RF signal, demodulates it, and sends the data stream to the microprocessor, which decodes it and sends commands to the command module. Almost all RF receivers have an output pin that can record the voltage as a function of the input receiver power. Figure 2 shows the calibration function between the signal generator power-injected into the RF receiver input (a typical RKE receiver from Infineon), and the output receiver voltage.

3. SIGNAL AND NOISE MEASUREMENTS PROCEDURE

The RKE system test setup is shown in Figure 3. This system uses an external antenna installed separately from the RF module under the front dashboard. Tests are performed at a distance $R = 100$ m between the transmitter and the vehicle. The CW transmitter provides an effective radiated power equal to -12 dBm. (-12 dBm is the FCC upper-power limit for 315-MHz frequency). The 315-MHz frequency-range signal has a horizontal polarization. The RKE receiver, together with the microprocessor and command

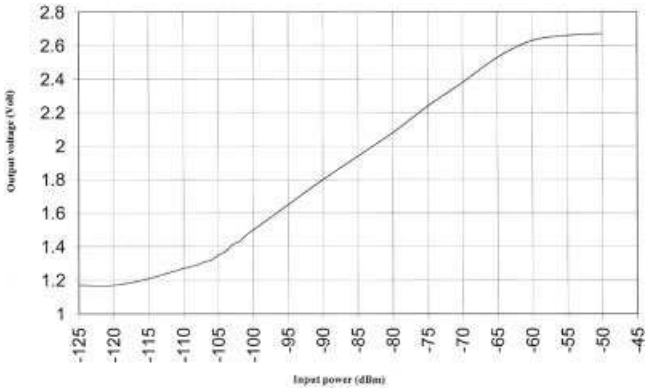

Figure 2 Calibration curve between the RF power injected to RF receiver TDA 5211 (from Infineon) and output-voltage level

circuit, is located on the steering column and is connected to the active antenna via the RF cable. The car, together with the RKE system, is positioned on an outdoor automobile turntable. A receiver output data point is taken every 2° as the turntable is rotated through a full 360° azimuth. The antenna-range instrumentation is controlled by a computer that drives the turntable rotation and transfers measured data to the hard drive and printer.

4. MEASUREMENT RESULTS

A Durango 2004 (Chrysler) vehicle was chosen as the base vehicle for the measurements. As a preliminary step, the noise level received by the RF receiver was measured with an active antenna and found to be 1.35 V. According to the calibration curve, this value corresponds to a noise-power level at the receiver input of −102.5 dBm. This latter value is the total noise level, and includes the thermal noise of the antenna amplifier as well as noise received by the antenna from the surrounding environment, including car-equipment noise and receiver thermal noise. The thermal noise for an antenna amplifier can be calculated from Eq. (3), with the equivalent bandwidth of the measuring device taken as 300 KHz. Laboratory measurements revealed that the antenna amplifier gain is equal to 15 dB and the amplifier noise figure is 2 dB. The noise value at the receiver input is then −103.5 dBm. The receiver thermal-noise floor (from Infineon) is much less than −103.5 dBm.

It is possible to estimate which noise source—thermal or external—contributes to the bulk of the overall noise value. The total measured noise, −102.5 dBm, is the sum of the thermal noise equal to −103.5 dBm and an external noise. In this fashion, it can be seen that the thermal noise of the active antenna prevails over the external noise.

Signal levels were measured when the car on the turntable was being rotated more than 360°. Under "real life" as well as laboratory conditions, the gain of the antenna in the vehicle, and consequently the signal at the RF output, is not well-controlled, and varies as a function of relative car orientation. Therefore, an acceptable practice for microradio automotive applications is to measure the signal at various antenna orientations relative to the transmitter position, and then to present the signal variations as a statistical chart. A measured statistical histogram is shown in Figure 4. The histogram shows the relationship between voltage level and the data count with a certain voltage level (expressed as a percentage of total data points). The dashed vertical line shows the voltage level (1.57 V) for which the input RF power (−92.5 dBm) is above the noise level by 10 dB: this signal value provides a probability of detection of 0.99, as our example has specified. The histogram chart shows that 97% of the measured values are above the threshold of 1.57 V. This means that the RKE system has to detect the signal for 97% of the vehicle-angle positions if a person who is activating this system is 100 m away from the car. A field experiment with an RKE system showed 95% successful communication between the fob key and the RKE module (successfully opening or closing the car door).

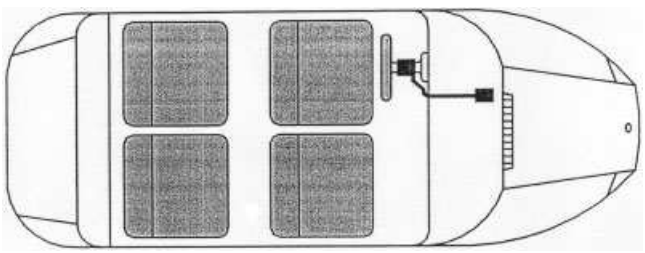

Figure 3 RKE system in situ on the vehicle

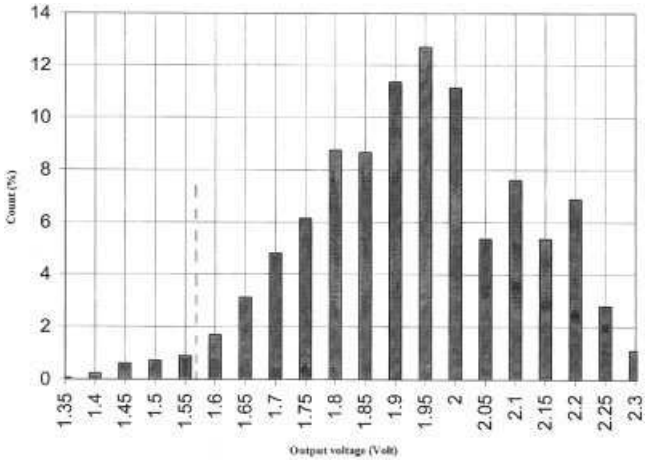

Figure 4 Measured voltage-data number as a function of the specified measured voltage level (statistical distribution of the output-voltage level)

During the field experiment, a person with a fob key was located 100-m distant from the turntable. The vehicle with the RKE system was located on the turntable. While the turntable was caused to rotate more than 360°, the person 100-m distant from the car periodically pushed the fob-key button, hence transmitting the signal for opening the car door. A second person in the car calculated the number of successful openings. The ratio of successful door openings to the total fob-key button pushes determined the percentage of successful communications between the fob key and the RKE module. As can be seen from Figure 4, the field experiment with the fob-key button and the estimation according to the described test procedure are in good agreement.

A second set of measurements were conducted to explore the situation when the external noise exceeded the thermal noise. For these purposes, we placed a wideband jammer in the car. This jammer increased the voltage level at the receiver output to 1.9 V. This value corresponds to a noise-power value at the receiver input equal to −86 dBm. Therefore, the threshold level for stable RKE operation ($q_0 = 10$ dB) increases to 2.2 V (−76 dB). According to the histogram graph, only 11% of the angle-measured points are above 2.6 V. Laboratory measurements of the RKE system showed 7% successful transmission.

A practically useful graph shown in Figure 5 allows for estimation of an RKE system range as a function of the voltage

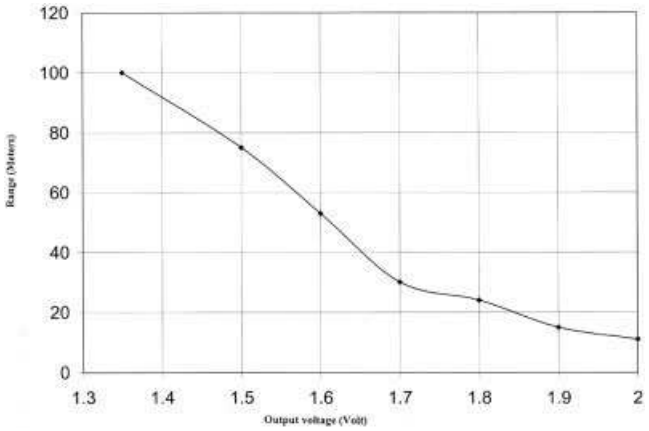

Figure 5 Relationship between the noise voltage and RKE system range

measurements at the receiver output. The curve shown reveals the relationship between the noise-voltage level and the system range (the system provides for more than 97% successful transmission over 360° around the car).

5. CONCLUSION

A measurement procedure for signal and noise estimation of an RKE system in a vehicle using an active antenna and an RF receiver has been proposed. Using this procedure, the signal and noise of an RKE module in a car in a noisy environment can be measured at the required range. Range estimation based on the test data, according to the described test procedure, was confirmed by laboratory experiments with a remote-control module. We can conclude that such a measurement procedure will be useful in helping to design a properly operating RKE system.

REFERENCES

1. F.L. Dacus, Design of short range radio systems, Microwaves RF 40 (2001), 73–80.
2. A. Bensky, Short-range wireless communications, LLH Technology Publishing, 2000.
3. J. Salter, Specifying UHF active antennas and calculating system performance, Research & Development British Broadcasting Corporation, White Paper 066, 2003.
4. A. Bensky, Range estimation for short-range event transmission systems, RF Design (2002), 30–38.
5. G.W. Milne, E.J. Jansen, J.J. Roux, J. Koekemoer, and P.A. Kotze, EMC and RFI problems and solutions on the SUNSAT micro-satellite, South African Symp Commun Signal Processing, Cape Town, South Africa, 1998, pp 293–298.
6. B. Al-Khateeb, V. Rabinovich, and B. Oakley, An active receiving antenna for short-range wireless automotive communication, Microwave Opt Technol Lett 44 (2004), 200–205.

INVESTIGATION OF MICROSTRIPLIKE MODE SUPPRESSION IN UC-PBG FW-CBCPW BY USING AN ELECTRO-OPTIC NEAR-FIELD CHARACTERIZATION

K.-H. Oh,[1] H.-J. Song,[1] S. Moon,[1] T.-Y. Kim,[1] G. Mudhana,[1] W. B. Kim,[2] D.-Y. Kim,[1] and J.-I. Song[1]
[1] Department of Information and Communications
Gwangju Institute of Science and Technology
1 Oryong-dong, Buk-gu
Gwangju, 500-712, Korea
[2] Department of Electrical Engineering
Songwon College
199-1 Gwangchun-dong Seo-gu
Gwangju, Korea

Received 13 April 2005

ABSTRACT: *Near-field patterns of uniplanar compact photonic bandgap (UC-PBG) and non-UCPBG finite-width conductor-backed coplanar waveguides (FW-CBCPWs) are characterized using an electro-optic near-field mapping system. This system is very effective in visually showing the role of the UC-PBG structure in the suppression of microstriplike (MSL) modes in the FW-CBCPWs.* © 2005 Wiley Periodicals, Inc. Microwave Opt Technol Lett 47: 119–122, 2005; Published online in Wiley InterScience (www.interscience.wiley.com). DOI 10.1002/mop.21098

Key words: *electro-optic near-field characterization; FW-CBCPW; MSL mode; UC-PBG*

INTRODUCTION

Circuits based on coplanar waveguides (CPWs) offer advantages, including an easy parallel and series access of passive and active components without using via holes, as compared to those based on microstrip lines. However, special care must be taken to avoid the effects of undesired propagation modes when broadband performance is required. In finite-width conductor-backed coplanar waveguides (FW-CBCPWs), there are two dominant modes, CPW and microstriplike (MSL) modes, having no cutoff frequencies, as illustrated in Figure 1 [1, 2]. Thus, unless certain mode-suppression techniques are employed, undesirable MSL modes, including higher-order resonance modes, may be excited and propagate along the structures, resulting in circuit-performance deterioration. The resonance peaks observed in the *S*-parameter measurements of the FW-CBCPWs are related to the excitation of extra higher-order modes (in the form of the MSL mode), which are supported by the 2D resonator formed by finite-width side-ground plates on both sides of the center signal-strip [2]. The conventional method to suppress the MSL mode in FW-CBCPWs was to use via holes to connect the two side-ground plates to the bottom-ground plate [3]. However, this method complicates the fabrication process. A photonic bandgap (PBG) structure, called an uniplanar compact photonic bandgap (UC-PBG) structure, has been reported to efficiently suppress the MSL mode in FW-CBCPWs and thus improves the transmission characteristics without losing the advantages of CPWs [4, 5]. Verification of the MSL mode suppression utilizing the novel PBG structure in FW-CBCPWs was carried out by using computer-aided simulations or *S*-parameter measurements. However, the computer-aided simulations provide field distributions obtained from theoretical analysis of idealized microwave circuit structures, and the *S*-parameter measurements can provide only an indirect indication of MSL mode suppression inferred from the difference in *S*-parameters of the conventional non-UC-PBG and